PULSE REPETITION INTERVAL ESTIMATION IN MOVING PASSIVE SENSORS BASED ON OBSERVATION CALIBRATION

H. H. Ye[*], Z. Liu, and W. L. Jiang

College of Electronic Science & Engineering, National University of Defense Technology, Changsha 410073, China

Abstract—High-accuracy pulse repetition interval (PRI) estimation is meaningful for passive sensors to identify radar emitters. This paper considers the problem of estimating the PRIs of motionless radars in moving passive sensor systems. A modified method which based on observation calibration is proposed. This method can efficiently compensate the estimation bias induced by model mismatch, through calibrating the pulse time of arrival (TOA) measurements with emitter geolocation information. Performance analysis and simulation results show that our method can improve the PRI estimation accuracy significantly.

1. INTRODUCTION

Radar is an instrument that radiates electromagnetic waves is space and detects the presence and location of objects from the reflected waves [1–3]. Passive sensors, such as electronic intelligence (ELINT) and electronic support measures (ESM) systems, represent a class of important military sensors [4, 5], which intercept and analysis the electromagnetic waves transmitted by radars to obtain information about their capabilities. Because radars are mostly used for purpose of remote sensing [6], passive sensors are also treated as the remote sensors of remote sensors [7]. Nowadays, with the advancements of radar technologies and the rapid deployment of vast radar units, modern passive sensors confront ever more dense and complex emitter environments [8]. Under this circumstance, an advanced technology called specific emitter identification (SEI) was proposed to

distinguish different radars. SEI identifies individual radars by using the signal fingerprint features produced by the unideal components in transmitters [7, 8]. The radar pulse repetition interval (PRI) has been found to been an important fingerprint parameter, because it reflects the period of the timer which controls pulse generation, and any group of timers exhibits small differences in the mean period among its members [7, 8]. Therefore, accurate PRI estimation is quite meaningful for radar SEI.

The problem of accurate PRI estimation was firstly studied in [9], where it was modeled as period estimation of a periodic point process. Recent years, this problem has attracted many attentions due to the increasing requirements of SEI [10–13]. A refined modified Euclidean algorithm (MEA) was proposed in [10] for the circumstance when there is not much prior knowledge of the range of the period. In [11] an estimator called the separable least squares line search (SLS2-ALL) was proposed, to search a quasi-maximum likelihood estimate (MLE) of the sought PRI. Clarkson studied the problem based on lattice theory and proposed a lattice line search (LLS) algorithm [12], which also can not ensure yielding a MLE, however. Most recently, the maximum likelihood (ML) estimation of the PRI was realized by McKilliam and Clarkson in [13], where an estimator called the *integer lattice line search* (ZnLLS) was proposed.

The above mentioned studies focus on the ML estimation of PRI based on the periodic point process model, which implicitly requires that there is no relative movement between the passive sensor and the intercepted radar. In practice, there are many passive sensors which are mounted on moving platforms such as aircrafts or satellites [5]. Due to platform motion, the data measurements inevitably dissatisfy the static observation model. However, as far as we are aware, existing studies have investigated neither the impact of the relative movement on the PRI estimation nor the way to eliminate it.

In this paper, we will study the PRI estimation for moving passive sensors. In Section 2, the moving observation model is derived based on an assumption that the platform moves in a linear and uniform-speed manner. Section 3 analyzes the estimation bias caused by model mismatch, and presents a modified PRI estimation method which is based on observation calibration. The performance is validated with numerical simulation in Section 4, followed by the conclusions in the last section.

2. MOVING OBSERVATION MODEL

2.1. Static Observation Model and the Maximum Likelihood Estimation

Using the Dirac delta function, the time of arrival (TOA) measurements of a set of received pulses can be modeled as the following point process signal [9]:

$$z(t) = \sum_{i=0}^{n-1} \delta\left(t - t_i\right) \tag{1}$$

where t_i is the TOA measurements of the ith pulse. For a passive sensor mounted on a motionless platform, the expression of t_i is given by [9–13]

$$t_i = \bar{t}_0 + k_i\, T + \varepsilon_i, \qquad i = 0,\, \ldots,\, n-1 \tag{2}$$

where T represents the radar PRI; $\bar{t}_0$ is the exact TOA of the first pulse; ε_i's are the white Gaussian noises with variance σ^2; k_i's are integers with k_0 fixed at 0. If the observations are complete without pulse missing, then $k_i = i$ and $z(t)$ would be a complete periodic point process [14]. However, in practice, due to a range of intercept difficulties [7], pulse missing happens commonly. Under this condition, PRI estimation is modeled as a problem of estimating the period of a periodic point process from incomplete and noisy data [10–13].

The difficulty of this problem arises from the fact that both the integer set $\{k_i\}_{i=0}^{n-1}$ and the period T are unknown. Fortunately, after plenty of studies (see e.g., [9–13] and the references therein), it has been proved in [13] that the maximum likelihood estimation of T can be realized based on an estimator called the the *integer lattice line search* (ZnLLS). In addition, it has also been shown that under the condition that the ratio T/σ is larger than a certain threshold (typically be about 10), the MLE of T can attain the so called 'clairvoyant Cramer-rao lower bound (CRLB)', which is given by [11]

$$\mathrm{var}\left(\widehat{T}\right) = \frac{n\sigma^2}{n\sum_{i=0}^{n-1} k_i^2 - \left(\sum_{i=0}^{n-1} k_i\right)^2} = \frac{\sigma^2}{2\sum_{i=0}^{n-2}\sum_{j=i+1}^{n-1}\left(k_j - k_i\right)^2} \triangleq B_s \tag{3}$$

where $\widehat{T}$ denotes the MLE of T, and B_s defines the bound. The bound B_s is clairvoyant in the sense that it is derived under an assumption that the exact $\{k_i\}_0^{n-1}$ is known. When $\widehat{T}$ attains the CRLB, it satisfies

the following relation [11]

$$\widehat{T} = \widehat{T}_{\text{clair}} = \frac{\sum\limits_{i=0}^{n-2} \sum\limits_{j=i+1}^{n-1} (k_j - k_i)(t_j - t_i)}{\sum\limits_{i=0}^{n-2} \sum\limits_{j=i+1}^{n-1} (k_j - k_i)^2} \tag{4}$$

where $\widehat{T}_{\text{clair}}$ is the MLE of T under the same assumption that the $\{k_i\}_{i=0}^{n-1}$ is known. Here we call $\widehat{T}_{\text{clair}}$ the 'clairvoyant MLE'.

It should be stressed that one can not estimate the T by directly making use of (4) because in practice the set $\{k_i\}_{i=0}^{n-1}$ is unknown. We just use this equation to show that the MLE $\widehat{T}$ yielded by the estimator ZnLLS will be equal to $\widehat{T}_{\text{clair}}$, as long as T/σ is larger than the threshold.

Furthermore, because the accuracy of $\widehat{T}$ diverge from the CRLB rapidly as the ratio T/σ becomes smaller than the threshold, and inaccurate PRI estimation is meaningless for SEI, in this paper, we only consider the case when the MLE attains the CRLB. In fact, the radar PRI is normally larger than 100 microsecond (μs), while the TOA measurement noises are on the order of 10 nanoseconds (ns) [15], $T \gg \sigma$ and thus it is nature that $\widehat{T}$ attains the CRLB.
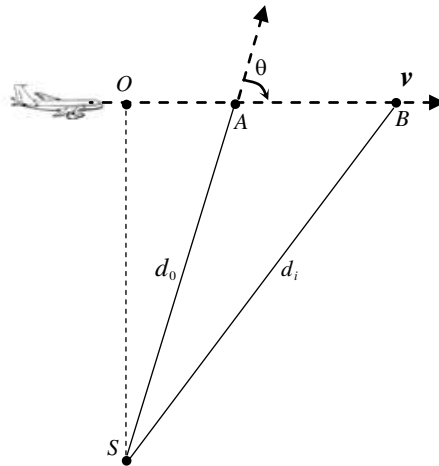
Figure 1. The scenario that a passive sensor mounted on an aircraft intercepts a motionless radar in a short time.

2.2. Moving Observation Model

During a short period of time (on the order of 1 second) within which a pulse train is received, the platform can be assumed to be move in the linear and uniform-speed manner. Fig. 1 depicts an aircraft that receives a pulse train transmitted from a motionless radar (located at the point S) during in a short time. The aircraft receives the first and the ith pulses at the times $\bar{t}_0$ and $\bar{t}_i$, and at the points A and B, respectively. Let $d_0 = \left|\overrightarrow{SA}\right|$ and $d_i = \left|\overrightarrow{SB}\right|$ denote the distances from the point S to the points A and B ($|\cdot|$ represents the length of a directed line segment), it follows that

$$\bar{t}_i = \bar{t}_0 + k_i T + \frac{d_i - d_0}{c} \tag{5}$$

with c representing the speed of light. Then the observation model (see (2)) can be replaced by

$$t_i = \bar{t}_0 + k_i T + \frac{d_i - d_0}{c} + \varepsilon_i \tag{6}$$

After extending the segment $\overrightarrow{AB}$ to the point O such that $\overrightarrow{SO} \perp \overrightarrow{OB}$, the difference of distance $d_i - d_0$ can be expressed by

$$
\begin{aligned}
d_i - d_0 &= \sqrt{\left(\left|\overrightarrow{OA}\right| + \left|\overrightarrow{AB}\right|\right)^2 + \left|\overrightarrow{SO}\right|^2} - \left|\overrightarrow{SA}\right| \\
&= \left|\overrightarrow{SA}\right| \left[\left(1 + 2\frac{\left|\overrightarrow{OA}\right|}{\left|\overrightarrow{SA}\right|}\frac{\left|\overrightarrow{AB}\right|}{\left|\overrightarrow{SA}\right|} + \frac{\left|\overrightarrow{AB}\right|^2}{\left|\overrightarrow{SA}\right|^2}\right)^{\frac{1}{2}}\right] - \left|\overrightarrow{SA}\right| \\
&= d_0 \left[\left(1 + 2\cos\theta\frac{\left|\overrightarrow{AB}\right|}{d_0} + \frac{\left|\overrightarrow{AB}\right|^2}{d_0^2}\right)^{\frac{1}{2}}\right] - d_0
\end{aligned} \tag{7}
$$

with θ denoting the angle between $\overrightarrow{AB}$ and $\overrightarrow{SA}$ such that $\cos\theta = \left(\overrightarrow{AB} \cdot \overrightarrow{SA}\right)\big/\left(\left|\overrightarrow{AB}\right|\left|\overrightarrow{SA}\right|\right)$ ('·' represents inner product operation). Define $x = \left|\overrightarrow{AB}\right|\big/d_0$, then x is close to 0, because $\left|\overrightarrow{AB}\right| \ll d_0$, under the remote sensing conditions. Substituting this expression of x into (7) and then expanding it in terms of its second Taylor expansion, we

get

$$d_i - d_0 = d_0 \left(x \cos \theta \right) + \frac{d_0}{2} \left(x \sin \theta \right)^2$$

$$= \left| \overrightarrow{AB} \right| \cos \theta + \frac{1}{2d_0} \left(\left| \overrightarrow{AB} \right| \sin \theta \right)^2 \tag{8}$$

Furthermore, let $\mathbf{v} = [v_x, v_y, v_z]^T$ (the superscript 'T' represents transposition) denote the velocity vector of the platform and $\|\mathbf{v}\|$ denote the speed value, and define $v_R = \|\mathbf{v}\| \cos \theta$ as the value of the radial velocity (i.e., the component of $\mathbf{v}$ along the direction of $\overrightarrow{SA}$), and $v_T = \|\mathbf{v}\| \sin \theta$ as the value of tangential velocity, then
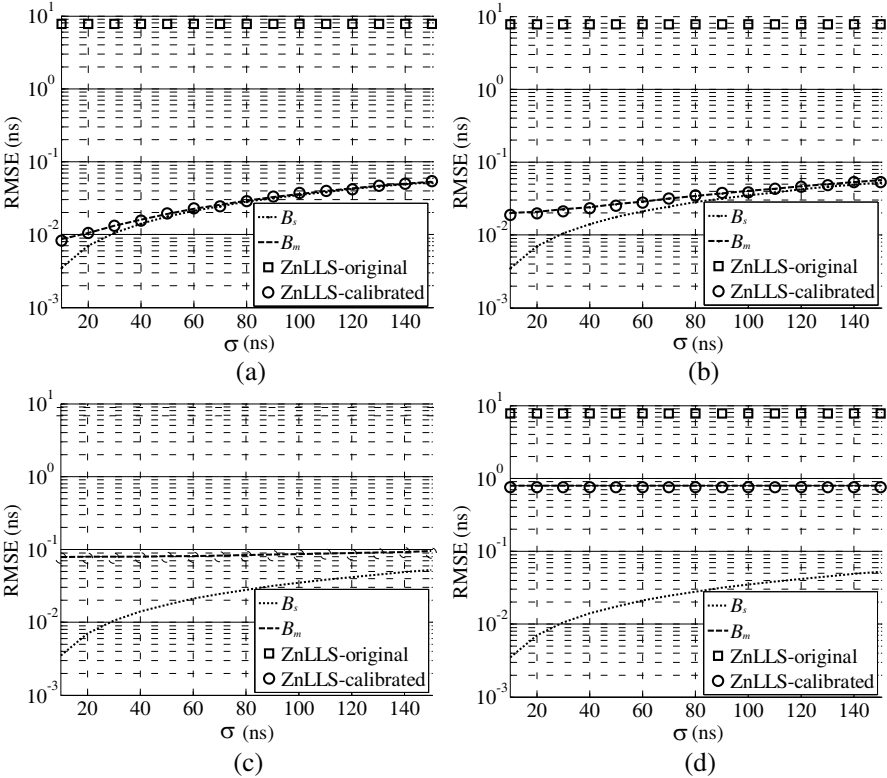
Figure 2. Comparison of the PRI estimations with original and calibrated observations. (a) $\sigma_s = 0.2\,\mathrm{km}$. (b) $\sigma_s = 0.5\,\mathrm{km}$. (c) $\sigma_s = 2\,\mathrm{km}$. (d) $\sigma_s = 20\,\mathrm{km}$.

$\left|\overrightarrow{AB}\right| = \|\mathbf{v}\| \, (\bar{t}_i - \bar{t}_0)$ and (8) can be replaced by

$$d_i - d_0 = v_R \, (\bar{t}_i - \bar{t}_0) + \frac{[v_T \, (\bar{t}_i - \bar{t}_0)]^2}{2 \, d_0} \qquad (9)$$

Define $d_R = v_R \, (\bar{t}_i - \bar{t}_0)$ and $d_T = v_T \, (\bar{t}_i - \bar{t}_0)$ to represent the radial and tangential displacements of the platform respectively, then $d_i - d_0 = d_R + (d_T/2) \, (d_T/d_0)$. Because $d_T < \left|\overrightarrow{AB}\right| \ll d_0$, it is easy to see that the variation of signal transmission distance is mainly due to the radial movement of the platform.

Combining (6) and (9), the moving observation model is further expressed by

$$t_i = \bar{t}_0 + k_i T + \frac{v_R}{c} \, (\bar{t}_i - \bar{t}_0) + \frac{v_T^2 \, (\bar{t}_i - \bar{t}_0)^2}{2 c d_0} + \varepsilon_i, \qquad i = 0, \ldots, n-1 \quad (10)$$

Let $\mathbf{s} = [x, y, z]^T$ and $\mathbf{s}_a = [x_a, y_a, z_a]^T$ denote the position coordinates of the points S and A respectively, then the variables d_0, v_R and v_T^2 in (10) can be calculated by using

$$d_0 = \left|\overrightarrow{SA}\right| = \|\mathbf{s} - \mathbf{s}_a\| \qquad (11)$$

$$v_R = \|\mathbf{v}\| \cos\theta = \frac{\mathbf{v}^T \, (\mathbf{s} - \mathbf{s}_a)}{\|\mathbf{s} - \mathbf{s}_a\|} \qquad (12)$$

$$v_T^2 = \|\mathbf{v}\|^2 \sin^2\theta = \|\mathbf{v}\|^2 - \frac{\left(\mathbf{v}^T \, (\mathbf{s} - \mathbf{s}_a)\right)^2}{\|\mathbf{s} - \mathbf{s}_a\|^2} \qquad (13)$$

3. CALIBRATION OF THE PRI ESTIMATION

3.1. Necessity of Calibration

For a moving passive sensor, if the PRI of an intercepted radar is estimated by using the moving observation set $\{t_i\}_{i=0}^{n-1}$ directly without calibration, bias would be induced by the reason of model mismatch. This subsection analyzes this estimation bias. As it was stressed above, we only consider the case when the MLE attains the CRLB, then the MLE of T has the value as shown in (4).

From (10), the difference of the exact TOA measurements of the ith and jth pulses is given by

$$\bar{t}_j - \bar{t}_i = (k_j - k_i) \, T + \frac{v_R}{c} \, (\bar{t}_j - \bar{t}_i) + \frac{v_T^2}{2 \, c d_0} \, (\bar{t}_j + \bar{t}_i - 2\bar{t}_0) \, (\bar{t}_j - \bar{t}_i) \quad (14)$$

i.e.,

$$\bar{t}_j - \bar{t}_i = \frac{(k_j - k_i)\,T}{1 - \dfrac{v_R}{c} - \dfrac{v_T}{c}\dfrac{v_T\,(\bar{t}_j - \bar{t}_0) + v_T\,(\bar{t}_i - \bar{t}_0)}{2\,d_0}} \tag{15}$$

Because the speed of the platform is much smaller than the light speed (i.e., $v_R \ll c$ and $v_T \ll c$), and the tangential displacements $v_T\,(\bar{t}_i - \bar{t}_0)$ and $v_T\,(\bar{t}_j - \bar{t}_0)$ are both much smaller than the distance d_0, we have $\bar{t}_j - \bar{t}_i \approx (k_j - k_i)\,T$. Substituting this relation into the right hand side of (15) yields

$$\bar{t}_j - \bar{t}_i \approx (k_j - k_i)\,T \left[1 + \frac{v_R}{c} + \frac{v_T^2\,(k_j + k_i)\,T}{2\,c\,d_0} \right] \tag{16}$$

Combining (4) and (16), we get the estimation bias as follows

$$\mathrm{bias}\left(\widehat{T}\right) = E\left(\widehat{T}\right) - T$$

$$\approx \frac{v_R}{c}T + \frac{v_T^2 T^2}{2cd_0}\frac{\displaystyle\sum_{i=0}^{n-2}\sum_{j=i+1}^{n-1}(k_j + k_i)(k_j - k_i)^2}{\displaystyle\sum_{i=0}^{n-2}\sum_{j=i+1}^{n-1}(k_j - k_i)^2}$$

$$\triangleq\ b_R + b_T \tag{17}$$

where b_R and b_T are defined to represent the corresponding biases caused by radial and tangential movements respectively.

The bias shown above is typically much larger than the estimation error caused by TOA measurement noises. To show this, we assume a Bernoulli pulse missing model with a parameter p, like that in [10–13]. Under this assumption, k_i is expected to be about i/p, and the pulse missing rate is expected be about $1 - p$ [10]. Typically, we assume that the PRI $T = 1$ millisecond (ms), the noise standard deviation $\sigma = 5 \times 10^{-5}$ ms, $p = 0.1$ and the total observation time is about 1 second (s) (thus k_{n-1} is about 1000). Under these conditions, from (3) one can find out that the root mean square error (RMSE) caused by the noise is on the order of 10^{-8} ms, i.e., $\sigma\left(\widehat{T}\right) \approx O\left(10^{-8}\right)T$. As an example, if the platform is a satellite, then its speed $\|\mathbf{v}\|$ is typically about $7.8\,\mathrm{km/s}$, and its distance to a radar on the ground is typically longer than hundreds of kilometers (km). Under the above conditions, from (17) we can have that $b_R = O(10^{-5})T$ and $b_T = O(10^{-7})T$, which are both much larger than $\sigma\left(\widehat{T}\right)$. Therefore, the bias must be compensated.

3.2. Method of Calibration

Comparing the moving observation model (see (10)) to the static observation model (see (2)), we see that if the moving observation t_i is calibrated using

$$t'_i = t_i - \frac{v_R}{c}(\bar{t}_i - \bar{t}_0) - \frac{1}{2\,c\,d_0}\,v_T^2\,(\bar{t}_i - \bar{t}_0)^2 \qquad (18)$$

then the calibrated observations t'_i's agree with the static observation model. In (18), the $\bar{t}_0$ and $\bar{t}_i$ are both real TOA values, which are impossible to know exactly. Since the radar PRI is normally significantly larger than the TOA measurement noises [15], we have $\bar{t}_i - \bar{t}_0 \gg |\varepsilon_i - \varepsilon_0|$, and thus

$$\bar{t}_i - \bar{t}_0 = (t_i - \varepsilon_i) - (t_0 - \varepsilon_0) \approx t_i - t_0 \qquad (19)$$

i.e., the $\bar{t}_i - \bar{t}_0$ in (18) can be replaced by $t_i - t_0$.

On the other hand, from (11) $\sim$ (13) we see that d_0, v_R and v_T can be obtained provided the position of the radar (i.e., the vector $\mathbf{s}$), the position of the platform at the time $\bar{t}_0$ (i.e., the $\mathbf{s}_a$) and the velocity vector $\mathbf{v}$ are all known. In practice, the position and velocity of the platform can be accurately obtained with the help of the carried navigation device, such as the global position system (GPS). In addition, since a passive sensor normally has got the ability of emitter geolocation [4, 5], the position of the radar can be estimated with the emitter geolocation result. Therefore, we propose the following observation calibration based PRI estimation method for the moving passive sensors:

Step 1: Calibrate the original TOA observations by using the position and velocity information of the platform and the geolocation result of the observed radar emitter, according to (11)–(13) and (18)–(19), to yield the calibrated observation set $\{t'_i\}_{i=0}^{n-1}$.

Step 2: Estimate the PRI utilizing estimators such as the ZnLLS based on the calibrated set $\{t'_i\}_{i=0}^{n-1}$.

3.3. Performance Analysis

Because the position and velocity information of the platform obtained from the navigation system are very accurate, for simplicity, they are assumed to be known exactly. Then according to the moving observation model, only the geolocation error and the TOA measurement noises result in the PRI estimation error. Denote the geolocation error by $\Delta\mathbf{s} = [\delta_x, \delta_y, \delta_z]^T$, whose mean and covariance are $\mathbf{0}$ (a vector whose elements are all zeros) and $\mathbf{C}$ respectively.

From (11)–(13) and (18)–(19), we can get the calibrated observation t_i' expressed by

$$
\begin{aligned}
t_i'\left(\mathbf{s}+d\mathbf{s}\right) \ = \ & t_i - \frac{t_i - t_0}{c}\frac{\mathbf{v}^T\left(\mathbf{s}+d\mathbf{s}-\mathbf{s}_a\right)}{\|\mathbf{s}+d\mathbf{s}-\mathbf{s}_a\|} \\
& - \frac{\left(t_i-t_0\right)^2}{2c}\left(\frac{\|\mathbf{v}\|^2}{\|\mathbf{s}+d\mathbf{s}-\mathbf{s}_a\|} - \frac{\left(\mathbf{v}^T\left(\mathbf{s}+d\mathbf{s}-\mathbf{s}_a\right)\right)^2}{\|\mathbf{s}+d\mathbf{s}-\mathbf{s}_a\|^3}\right) \quad (20)
\end{aligned}
$$

Expanding $t_i'\left(\mathbf{s}+d\mathbf{s}\right)$ in terms of its first Taylor expansion [16], it follows that

$$
\begin{aligned}
t_i'\left(\mathbf{s}+d\mathbf{s}\right) \ \approx \ & t_i - \frac{v_R}{c}\left(t_i-t_0\right) - \frac{1}{2cd_0}v_T^2\left(t_i-t_0\right)^2 \\
& - \frac{t_i-t_0}{c}\left(d\mathbf{s}\right)^T\nabla_s f\left(\mathbf{s}\right) - \frac{\left(t_i-t_0\right)^2}{2c}\left(d\mathbf{s}\right)^T\nabla_s g\left(\mathbf{s}\right) \quad (21)
\end{aligned}
$$

where

$$
\nabla_s f(\mathbf{s}) \triangleq \frac{\partial}{\partial \mathbf{s}}\left(\frac{\mathbf{v}^T\left(\mathbf{s}-\mathbf{s}_a\right)}{\|\mathbf{s}-\mathbf{s}_a\|}\right) = \frac{1}{\|\mathbf{s}-\mathbf{s}_a\|}\left[\mathbf{v} - \frac{2\mathbf{v}^T\left(\mathbf{s}-\mathbf{s}_a\right)}{\|\mathbf{s}-\mathbf{s}_a\|^2}\left(\mathbf{s}-\mathbf{s}_a\right)\right] \quad (22)
$$

$$
\begin{aligned}
\nabla_s g\left(\mathbf{s}\right) &\triangleq \frac{\partial}{\partial \mathbf{s}}\left(\frac{\|\mathbf{v}\|^2}{\|\mathbf{s}-\mathbf{s}_a\|} - \frac{\left(\mathbf{v}^T\left(\mathbf{s}-\mathbf{s}_a\right)\right)^2}{\|\mathbf{s}-\mathbf{s}_a\|^3}\right) \\
&= \frac{\left(\mathbf{s}-\mathbf{s}_a\right)}{\|\mathbf{s}-\mathbf{s}_a\|^3}\left(3\left(\frac{\mathbf{v}^T\left(\mathbf{s}-\mathbf{s}_a\right)}{\|\mathbf{s}-\mathbf{s}_a\|}\right)^2 - \|\mathbf{v}\|^2\right) - \frac{2\mathbf{v}^T\left(\mathbf{s}-\mathbf{s}_a\right)\mathbf{v}}{\|\mathbf{s}-\mathbf{s}_a\|^3} \quad (23)
\end{aligned}
$$

According to the relation $t_i - t_0 \approx \left(\bar{t}_i - \bar{t}_0\right)$ and the expression for t_i (see (10)), $t_i'\left(\mathbf{s}+d\mathbf{s}\right)$ can be further expressed by

$$
\begin{aligned}
t_i'\left(\mathbf{s}+d\mathbf{s}\right) \ \approx \ & t_0 + k_i T + \varepsilon_i - \frac{\bar{t}_j-\bar{t}_0}{c}\left(d\mathbf{s}\right)^T\nabla_s f\left(\mathbf{s}\right) \\
& - \frac{\left(\bar{t}_j-\bar{t}_0\right)^2}{2c}\left(d\mathbf{s}\right)^T\nabla_s g\left(\mathbf{s}\right) \quad (24)
\end{aligned}
$$

For presentation simplicity, we assume that the geolocation error and the TOA measurement noises are uncorrelated to each other. From (4) and (24), we get the estimation variance as follows

$$
\mathrm{var}\left(\widehat{T}\right) = \frac{E\left[\left(\sum_{i=0}^{n-2}\sum_{j=i+1}^{n-1}\left(k_j-k_i\right)\left(t_j'-t_i'\right)\right)^2\right]}{\left(\sum_{i=0}^{n-2}\sum_{j=i+1}^{n-1}\left(k_j-k_i\right)^2\right)^2} \quad (25)
$$

where

$$t'_j - t'_i = (k_j - k_i)\,T + (\varepsilon_j - \varepsilon_i) - \frac{\bar{t}_j - \bar{t}_i}{c}\,(d\mathbf{s})^T\,\nabla_s f\,(\mathbf{s})$$
$$- \frac{(\bar{t}_j - \bar{t}_i)^2}{2c}\,(d\mathbf{s})^T\,\nabla_s g\,(\mathbf{s}) \qquad (26)$$

Using the relation $\bar{t}_j - \bar{t}_i \approx (k_j - k_i)\,T$, (26) can be further replaced by

$$t'_j - t'_i = (k_j - k_i)\,T + (\varepsilon_j - \varepsilon_i) - \frac{(k_j - k_i)\,T}{c}\,(d\mathbf{s})^T\,\nabla_s f\,(\mathbf{s})$$
$$- \frac{((k_j - k_i)\,T)^2}{2c}\,(d\mathbf{s})^T\,\nabla_s g\,(\mathbf{s}) \qquad (27)$$

Substituting (27) into (25), the estimation variance becomes

$$\mathrm{var}\left(\widehat{T}\right) = B_s + B_R + B_T \qquad (28)$$

where B_s is the bound shown by (3), which is caused by the TOA measurement noises ε_i's, and B_R and B_T are the corresponding error terms for the radial and tangential movements respectively, which are shown as follows

$$B_R = \frac{T^2}{c^2}\,(\nabla_s f\,(\mathbf{s}))^T\,\mathbf{C}\,(\nabla_s f\,(\mathbf{s})) \qquad (29)$$

$$B_T = \frac{T^4}{4\,c^2}\left(\frac{\sum\limits_{i=0}^{n-2}\sum\limits_{j=i+1}^{n-1}(k_j - k_i)^3}{\sum\limits_{i=0}^{n-2}\sum\limits_{j=i+1}^{n-1}(k_j - k_i)^2}\right)^2\,(\nabla_s g\,(\mathbf{s}))^T\,\mathbf{C}\,(\nabla_s g\,(\mathbf{s})) \qquad (30)$$

When $\mathbf{C} = \sigma_s^2\mathbf{I}$ ($\mathbf{I}$ is the identity matrix), from (22)–(23) and (29)–(30), we have

$$B_R = \frac{\|\mathbf{v}\|^2}{c^2}\frac{\sigma_s^2}{d_0^2}T^2 \qquad (31)$$

$$B_T = \frac{T^4}{4c^2}\left(\frac{\sum\limits_{i=0}^{n-2}\sum\limits_{j=i+1}^{n-1}(k_j - k_i)^3}{\sum\limits_{i=0}^{n-2}\sum\limits_{j=i+1}^{n-1}(k_j - k_i)^2}\right)^2\frac{\left(\|\mathbf{v}\|^2 + 3v_R^2\right)v_T^2}{d_0^4}$$
$$< \frac{(v_T k_{n-1}T)^2}{d_0^2}\frac{\left(\|\mathbf{v}\|^2 + 3v_R^2\right)}{4\,c^2}\frac{\sigma_s^2}{d_0^2}T^2 \qquad (32)$$

Normally the geolocation error is much smaller than the remote sensing distance and the relative geolocation error σ_s/d_0 is typically on the

order of 1%. Under this condition, by comparing B_R and B_T with b_R and b_T (see (31) $\sim$ (32) and (17)), it is easy to see that the model bias can be significantly reduced.

Furthermore, since $v_T k_{n-1} T \ll d_0$ and $v_R^2 < \|\mathbf{v}\|^2$, from (31) and (32) we know that $B_R \ll B_T$. Then the estimation variance (28) can be approximated as

$$\mathrm{var}\left(\widehat{T}\right) \approx B_s + B_r \triangleq B_m \tag{33}$$

It is easy to see that B_s represents the corresponding theoretic error bound when the observations are perfectly (or exactly) calibrated, while B_m is the theoretic error bound for PRI estimation when the observations are calibrated with geolocation information.

4. SIMULATION RESULTS

As an example, we assume the platform of the passive sensor is a satellite whose orbit height and speed are about 600 km and 7.8 km/s respectively. When the sensor receive the first pulse, its position and velocity in the earth-fixed coordinate system are $(0.568, 6.912, 7.862) \times 10^6$ m and $(1.567, 0.746, 6.033) \times 10^3$ m/s respectively. The radar emitter is on the earth surface, it locates at a point whose coordinate is $(0.934, 6.344, 0.529) \times 10^6$ m. The total observation time is 1 s, the exact PRI is 1 ms, the integers k_i's are generated pseudorandomly from the Bernoulli model with $p = 0.1$. It means that the pulse missing rate is about 90% and 100 pulses are received in total. The covariance of the emitter geolocation can be written in the form of $\mathbf{C} = \sigma_s^2 \mathbf{I}$. Under these conditions, from (17) we can see that the theoretic bias will be on the order of 10 ns if the PRI is estimated directly based on the original observations.

Four sets of Monte Carlo simulations are performed to test the efficiency of the calibration against the geolocation error and the TOA measurement noise. The values of the σ_s for the four sets of trials are 0.2 km, 0.5 km, 2 km and 20 km respectively, and in each set of simulations, the TOA measurement noise standard deviation σ varies from 10 ns to 150 ns. PRI estimation errors are measured by root mean square error (RMSE). The theoretic bounds B_s and B_m are used as the benchmarks.

The experimental results are shown in Fig. 2, where 'ZnLLS-original' and 'ZnLLS-calibrated' represents the PRI estimates yielded by ZnLLS from the original and the calibrated observations respectively. As expected, it can be seen that PRI estimation without calibration leads bias which are significantly larger than B_s, which represents the estimation error induced by TOA measurement noises

or the corresponding theoretic error bound when the observations are perfectly calibrated, as it was pointed out. These estimation biases are shown to be obviously reduced after calibrating the observations. By comparing Figs. 2(a) $\sim$ (d), one can see that the efficiency of calibration depends upon the accuracy of the used emitter geolocation information, as expected. If the geolocation error is relatively too large (e.g., 2 km or larger), it will result in a dominant PRI estimation error. Under these cases, improving TOA measurement accuracy can not obviously reduce the estimation error (see Figs. 2(c) $\sim$ (d)). This shows the importance of accurate geolocation information for PRI estimation with moving observations. Furthermore, we can also see that the theoretical and simulated performance curves for the proposed method are almost overlapped under all the four cases, which validates result of theoretical performance analysis.

5. CONCLUSION

In this paper, a method was proposed for moving passive sensors to realize accurate emitter PRI estimation. By estimating the PRI from observations calibrated with emitter geolocation information, the proposed method was shown to achieve significant estimation error reduction with respect to estimation without calibration. Theoretic analysis and simulations have shown that the efficiency of the proposed method relies on the accuracy of the used emitter geolocation information, which suggests us to improve geolocation accuracy to enhance the PRI estimation performance in moving passive sensors.

ACKNOWLEDGMENT

REFERENCES

1. Aly, O. A. M. and A. S. Omar, "Detection and localization of RF radar pulses in noise environments using wavelet packet transform and higher order statistics," *Progress In Electromagnetics Research*, Vol. 58, 301–317, 2006.

2. Jiang, T., S. S. Z. Qiao, and J. Huangfu, "Simulation and experimental evaluation of the radar signal performance of chaotic

signals generated from a microwave Colpitts oscillator," *Progress In Electromagnetics Research*, Vol. 90, 15–30, 2009.

3. Toribio, R. and J. Saillard, "Identification of radar targets in resonance zone: e-pulse techniques," *Progress In Electromagnetics Research*, Vol. 43, 39–58, 2003.

4. Ware, P. J. and J. B. Mcdowall, "The application of pulse analyzers in passive sensor systems," *Proc. IEEE 28th European Microwave Conference*, 560–565, 1998.

5. "New trends in ESM/ELINT airborne sensors," *Proc. IEEE 28th European Microwave Conference*, 552–559, 1998.

6. Li, G., H. Meang, X. Xia, and Y. Peng, "Range and velocity estimation of moving targets using multiple stepped-frequency pulse trains," *Sensors*, Vol. 8, 1343–1350, 2008.

7. Wiley, R. G., *ELINT: The Interception and Analysis of Radar Signals*, Artech House, Norwood, 2006.

8. Langley, L. E., "Specific emitter identification (SEI) and classical parameter fusion technology," *Proc. IEEE WESCON*, 28–30, 1993.

9. Fogel, E. and M. Gavish, "Parameter estimation of quasi-periodic sequences," *Proc. Int. Conf. Acoust., Speech, Signal Process.(ICASSP)*, 2348–2351, 1988.

10. Sadler, B. M. and S. D. Casey, "On periodic pulse interval analysis with outliers and missing observations," *IEEE Trans. Signal Process.*, Vol. 46, 2990–3002, 1998.

11. Sidiropoulos, N. D., A. Swami, and B. M. Sadler, "Quasi-ML period estimation from incomplete timing data," *IEEE Trans. Signal Process.*, Vol. 53, 733, 2005.

12. Clarkson, I. V. L., "Approximate maximum-likelihood period estimation from sparse, noisy timing data," *IEEE Trans. Signal Process.*, Vol. 56, 1779–1787, 2008.

13. Mckilliam, R. and I. V. L. Clarkson, "Maximum-likelihood period estimation from sparse, noisy timing data," *Proc. Internat. Conf. Acoust. Speech Signal Process.*, 3697–3700, 2008.

14. Cox, D. R. and P. A. W. Lewis, *The Statistical Analysis of Series of Events*, Chapman and Hall, London, 1966.

15. Schleher, D. C., *Electronic Warfare in the Information Age*, Artech House, Norwood, MA, 1999.

16. Meyer, C. D., *Matrix Analysis and Applied Linear Algebra*, Cambridge University Press, 2001.